



[Proceedings of the 7th International Conference on HydroScience and Engineering
Philadelphia, USA September 10-13, 2006 \(ICHE 2006\)](#)

[ISBN: 0977447405](#)

[Drexel University](#)
[College of Engineering](#)

Drexel E-Repository and Archive (iDEA)
<http://idea.library.drexel.edu/>

Drexel University Libraries
www.library.drexel.edu

The following item is made available as a courtesy to scholars by the author(s) and Drexel University Library and may contain materials and content, including computer code and tags, artwork, text, graphics, images, and illustrations (Material) which may be protected by copyright law. Unless otherwise noted, the Material is made available for non profit and educational purposes, such as research, teaching and private study. For these limited purposes, you may reproduce (print, download or make copies) the Material without prior permission. All copies must include any copyright notice originally included with the Material. **You must seek permission from the authors or copyright owners for all uses that are not allowed by fair use and other provisions of the U.S. Copyright Law.** The responsibility for making an independent legal assessment and securing any necessary permission rests with persons desiring to reproduce or use the Material.

Please direct questions to archives@drexel.edu

LARGE-EDDY SIMULATION OF TURBULENT OPEN-CHANNEL FLOW WITH FREE-SURFACE FLUCTUATIONS

Akihiko Nakayama¹, Tomohiro Matsumura² and Nobuyuki Hisasue³

ABSTRACT

Large-eddy simulations of open-channel flows with free-surface fluctuations have been conducted. The conventional HSMAC algorithm of Hirt & Cook(1972) is extended to incorporate the calculation of the motion of the free surface within the iteration cycle for computing the pressure and the velocity using the kinematic and the dynamic conditions to be satisfied on the free surface. This method of computing a moving free surface has been verified in a benchmark of two-dimensional standing wave flow. For the sub-grid scale model, the standard Smagorinsky model with near-wall damping is used. Its performance is verified in a fully developed open-channel flow over a smooth flat bed at a laboratory Reynolds number. Subcritical flow past a sudden drop is then simulated and the results indicate that the mean velocity distribution can be predicted very well but the turbulent stresses need improvement.

1. INTRODUCTION

Large-eddy simulation is proving as a useful method of simulating turbulent flows in simple geometries and of moderate Reynolds numbers (eg. Ferziger and Peric 1997). Its application to more complex flows in hydraulic engineering is becoming possible and attempts are being made by many researchers. Most of them, however, treat the free surface as a rigid slip surface and do not consider its motion. When the free surface fluctuation interacts with the turbulent motion underneath it such as in open-channel flows with high Froude numbers, it is important that the free surface fluctuation is treated together with the turbulent fluctuations of other quantities. The most serious limitation of the present-day LES methods is that it requires fine numerical grids near solid boundaries for an accurate simulation. In the present work, a relatively standard LES method, that is known to work when the near-wall flow is resolved to a good degree, is extended so that the fluctuating motion of the free surface can be computed as a part of the entire turbulent flow. The numerical method of calculating the free-surface is first verified in a non-turbulent flow and the entire turbulent flow simulation method is tested in the calculation of the basic fully developed channel flow, then it is applied to the prediction of a flow past a sudden drop in a channel at a laboratory-scale Reynolds number. The flow near the free surface, where

¹ Professor, Graduate School of Science and Technology, Kobe University, Kobe, 657-8501, JAPAN (Nakayama@kobe-u.ac.jp)

² Graduate Student, Department of Architectural & Civil Engineering, Kobe University, Kobe, 657-8501, JAPAN

³ Research Engineer, Electric Power Research Institute, Kansai Electric Power Industry, Amagasaki, 661-0974, JAPAN

the scales of motion are usually larger than that near the solid boundary at the bottom, is also assumed to be resolved sufficiently so that effects of smoothing the fluctuation in the flow and the boundary shape may be ignored.

2. NUMERICAL METHOD

The present calculation method solves the filtered momentum equations with the sub-grid scale stresses and the continuity equation for the filtered velocity components (u, v, w) and the pressure p assuming that the free surface deforms freely with the vanishing stress.

Computation of flows with free-surface is usually done by solving the advection equation for the position of the free surface or some function that is related to the free-surface position in addition to the usual velocity and pressure computation. Usually the free surface position is assumed fixed at the stage of flow velocity calculation. VOF (Hirt and Nichols 1981) and level-set methods (Sussman et al. 1994) are examples of such methods. Since the convection equation does not contain the diffusion terms, unless a turbulence model is used, stable numerical calculation with sufficient accuracy is difficult (eg. Yabe and Aoki 1991). The fact that there is a time lag between the time the velocity is calculated and the time when the position of the free-surface boundary is moved, can cause a problem of consistency with the time discretization. In the present calculation method, these problems are avoided by extending the conventional Highly-Simplified MAC (HSMAC, Hirt and Cook 1972) method in such a way that the position of the free surface is determined during the iterative solution of the pressure and the velocity components.

In the HSMAC algorithm, the momentum equations are explicitly advanced in time to obtain an intermediate velocity at the new time step. In the present calculation, a second-order Adams-Bashforth integration is used. The correct velocity and the pressure at the new time step are sought by making the continuity to be satisfied by an iterative procedure. To do this in a rectangular grid system that is used here, the divergence D^* for each cell is computed from the intermediate velocity components defined at the staggered positions and if it is not zero or not small enough, the pressure p at the cell center is corrected by δp given by

$$\delta p = -\omega \frac{D^*}{\Delta t (1/\Delta x^2 + 1/\Delta y^2 + 1/\Delta z^2)} \quad (1)$$

where Δt is the time increment, Δx , Δy , Δz are the cell widths and ω is the acceleration parameter. As the pressure is updated, the velocity components normal to each of the surrounding surfaces of the cell are corrected since the additional pressure gradient creates additional flow. The velocity component u in the x -direction at the right surface of the cell, for example, is corrected by

$$\delta u = \Delta t \frac{\delta p}{\Delta x} \quad (2)$$

If the free surface intersects the cell being considered, the total flux D' through the cell bounding surfaces except for the free surface is computed and the position of the free surface is moved according to the continuity equation

$$h^{n+1} = h^n + \Delta t D' / (\Delta x \Delta y), \quad (3)$$

where h^n and h^{n+1} are the vertical elevation of the free surface within the cell at the old and the new time steps, D' is the total flux through the side surfaces surrounding the cell. The pressure at the center of this cell is then calculated by applying one of the boundary conditions on the free surface that the pressure is zero. It is noted that this relation is not correct if the surface intersects the upper or lower cell surface. In these cases, all the cells containing the free surface in the same vertical column are combined to form one tall cell and the same relation is applied. This allows the method to handle steep slopes but not overturning waves. An additional advantage of the present iterative method is that the total fluid volume can be preserved within a specified small error since the equation for determining the free surface position is this conservation equation itself. This is particularly useful since a method like the level-set method requires some adjustment of the average position to keep the fluid volume constant.

3. VERIFICATION OF THE NUMERICAL METHOD

The above-described method has been verified through the calculation of a standing wave in a tank with vertical slip walls as shown in Figure 1. The approximate analytical solution with an assumption that the amplitude of the free surface fluctuation is small compared with the tank depth is

$$\eta(x,t) = a \sin kx \sin \sigma t - \frac{1}{2} a \varepsilon \coth kD \cos 2kx \left\{ \sin^2 \sigma t - \frac{3 \cos 2\sigma t + \tanh^2 kD}{4 \sinh^2 kD} \right\}, \quad (4)$$

where η is the free-surface position at time t and distance x from the wall, D is the mean depth, k and σ are wave number and the frequency, respectively and ε is the steepness factor. Figure 2 shows the calculated free surface shape after one period of oscillation for the case of $\varepsilon=0.3$. The calculated profile is close to the analytical solution. Figure 3 shows the time change of the wave height at $x=0$ for a few periods of oscillation

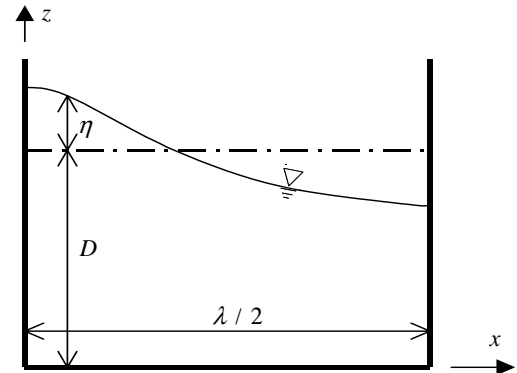


Figure 1 Standing wave as a test case.

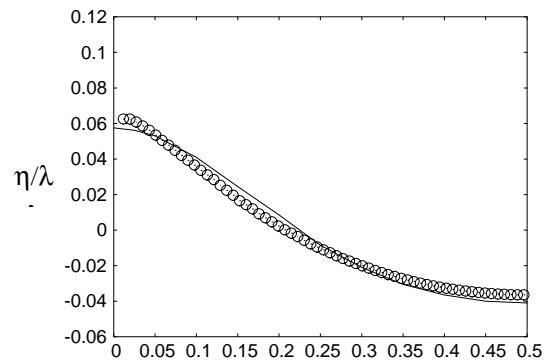


Figure 2 Free surface profile.
 , present cal.; , eq. 4.

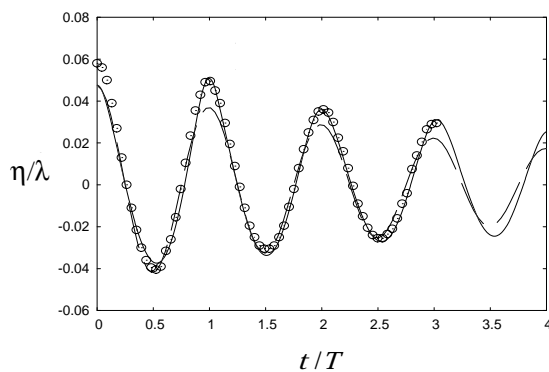


Figure 3 Results of wave height decay.
 , present cal.; --- theory, eq 4;. , Hodges and Street (1999).

compared with the analytical solution eq.4 and the computation by Hodges and Street (1999) obtained by using a free-surface conforming grid. It is seen that the rate of wave-amplitude decay agrees well with Hodges and Street calculation. This verifies that the present procedure does compute the free surface motion correctly.

4. TURBULENCE MODEL

The turbulence model for the sub-grid scale stress τ_{ij} makes use of the eddy viscosity assumption

$$\tau_{ij} = 2\nu_T S_{ij} \quad (5)$$

where ν_T is the eddy viscosity and S_{ij} is the component of the strain tensor of the filtered flow. The standard Smagorinsky model for ν_T

$$\nu_T = (C_S \Delta)^2 |S| \quad (6)$$

is used where Δ is the average grid size in the three directions and C_S is the Smagorinsky constant for which we take a value of 0.11. We assume that the near wall flow is reasonably resolved so that there are a few calculation points in the low-Reynolds-number region of the wall flow where the effective grid size is reduced by the Van Driest formula

$$\Delta = \sqrt[3]{\Delta x \Delta y \Delta z} (1 - \exp(-z^+ / 26)), \quad (7)$$

where z^+ is the viscous distance from the wall where the filtered velocity is assumed to satisfy the noslip condition. The dynamic Smagorinsky model in which the constant C_S is determined by test-filtering seems to be favored by many workers. The explicit filtering required in this procedure incurs additional computational time and does not necessarily improve the accuracy for comparable computational load (Nakayama and Vengadesan 2002). In the present writers' opinion, improvement in the results can be obtained by just increasing the grid resolution with similar increase in computational load.

The above model is more or less standard and has been applied in many flows but is verified here for fully developed open-channel flow with a constant bed slope. This flow with the bulk Reynolds number of 20,000 and the Froude number Fr of 1.2 has been calculated with a numerical grid of 55x45x115 points in the streamwise, crossflow and the vertical directions covering the flow region of $3H \times 2H \times H$, where H is the mean depth. With 115 points in the direction normal to the bottom wall the closest calculation point to the bottom is only a few times the viscous length.

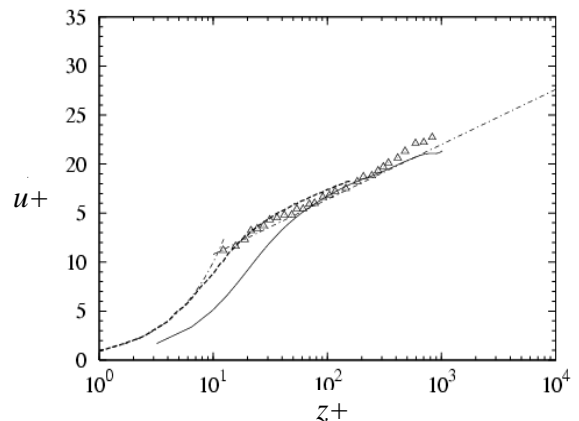


Figure 4 Mean velocity profile in fully developed channel flow with $Re=20,000$ and $Fr=1.23$. \bullet , present LES; $---$, DNS(Nakayama & Yokojima 2002); Δ , experiment(Nakayama 1997).

The calculation results are compared with the experimental data of Nakayama(1997) in Figures 4 and 5. In the mean-velocity plot of Figure 4, the DNS results of Nakayama and Yokojima (2001) are also shown for comparison though the Reynolds number is a little lower. The friction velocity U^* used to normalize the results is calculated from the channel slope. It is seen that, while the linear and the transition region are computed slightly lower than the experiment or the DNS, the present LES reproduces the logarithmic region very well. This means that the near-wall flow is not perfectly resolved. This can easily be cured by taking finer grid spacing near the bottom. What this figure shows is that reasonable results can be obtained with the first calculation point from the bottom of about three viscous units which allowed a high Reynolds number of 20,000 without an elaborate wall modeling. Figure 5 further shows that the Reynolds stresses are predicted fairly well but the present results show a stronger nonisotropy with larger streamwise fluctuation u' and smaller spanwise fluctuation v' and the vertical fluctuation w' , in particular within the first 10 to 20 percent of the channel depth. These are the same trends as seen in the prediction of a closed channel with similar resolution.

Near the free surface the fact that the vertical fluctuation reduces while the other fluctuations in the horizontal directions increase slightly is well known from previous experimental data of open-channel flows. Unlike most other calculations that use the free slip condition on the free surface, Figure 5 shows a vertical fluctuation of about $w'/U^*=0.1$. It is smaller than the experimental results of about 0.4, but the distribution across the entire channel is not very bad allowing for the under-prediction of the cross flow fluctuation. The present method, therefore, used computational grids of similar resolution or better of the near-wall flows, would give overall results that are acceptable.

5. CALCULATION OF FLOW OVER A DROP

The LES method described and verified in the previous sections has been applied to the simulation of flow over a backward-facing step in an open-channel and the results are discussed here. The flow configuration is depicted in Figure 6. Calculation has been conducted for two cases shown in Table 1. In the first case, Case1, the Froude number based on the mean velocity U_m and the mean depth h_0 is 0.42, and the flow remains subcritical throughout the computed domain while in the second case, the flow goes through the critical condition right downstream of the step, transitions to supercritical flow and then returns to subcritical flow after a weak hydraulic jump. In both cases the Reynolds number is fairly low and a good representation of the near wall flow can be achieved by not so fine grid. The flow upstream of the step is nearly a fully-developed uniform flow in the experiments with which the results are compared. In the calculation the inflow mean velocity profile at $x=x_m$ which is taken at 10 step heights upstream of the step, is assumed to take the standard logarithmic profile. As to the fluctuations,

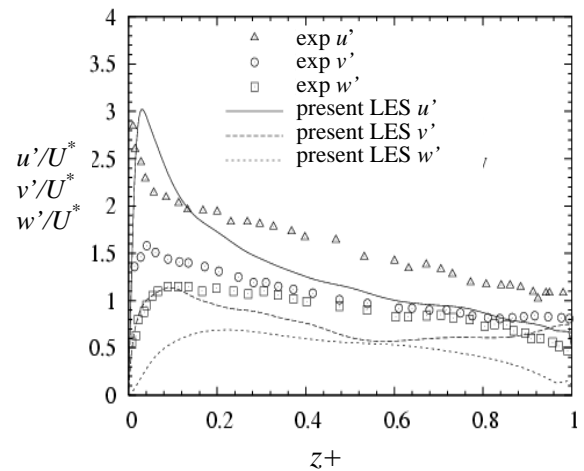


Figure 5 Turbulence intensity profile in fully developed channel flow with $Re=20,000$ and $Fr=1.23$. lines, present LES; symbols, experiment(Nakayama 1997).

Table1 Calculation cases.

Case	upstream $Re=U_m h_0/\nu$	Upstream Fr $U_m / \sqrt{gh_0}$	bed slope	upstream depth, h_0
Case1	4400	0.42	0.001	$2.2H_s$
Case2	5000	0.78	0.040	1.20

they are fed back from the downstream section where there are fully-turbulent fluctuations. Therefore, the inflow velocity components are set by

$$u(x_{in}, y, z, t) = \frac{u_{\hat{a}n}}{\kappa} \ln \frac{z u_{\hat{a}n}}{\nu} + B + u'(y, z, t), \quad (8)$$

$$v(x_{in}, y, z) = v'(y, z, t), \quad (9)$$

$$w(x_{in}, y, z) = w'(y, z, t), \quad (10)$$

where $u_{\tau in}$ is the bed shear stress at the inflow section, u' , v' , and w' are obtained from the fluctuation at the downstream outflow section, $x=x_{out}$ by rescaling it. For example u' is calculated as follows

$$u'(y, z, t) = \frac{u_{\hat{a}n}}{u_{\tau out}} u'(x_{out}, y, \frac{u_{\tau out}}{u_{\hat{a}n}} z, \frac{u_{\tau out}}{u_{\hat{a}n}} t - \Delta t), \quad (11)$$

where $u_{\tau in}$ and $u_{\tau out}$ are the mean friction velocities at the inflow and outflow sections.

The size of the numerical grid is 104x64x73 with few points above the highest expected free surface position. It can easily be handled by most work-station level computers.

Figure 7 compares the computed mean velocity profiles with the experimental results of Maruyama(2002) obtained by the PIV method. It is seen that the mean streamwise velocity component agrees very well with the measured results except in a small region just downstream of the step. It is likely that the PIV result could be influenced by reflection off the corner. Figure 8 shows the similar comparison of the calculated resolved turbulent kinetic energy k with the measured values. The

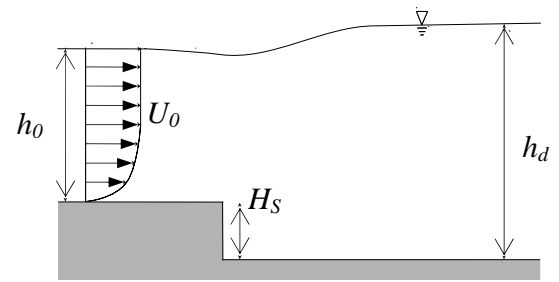


Figure 6 Configuration of flow past a sudden drop.

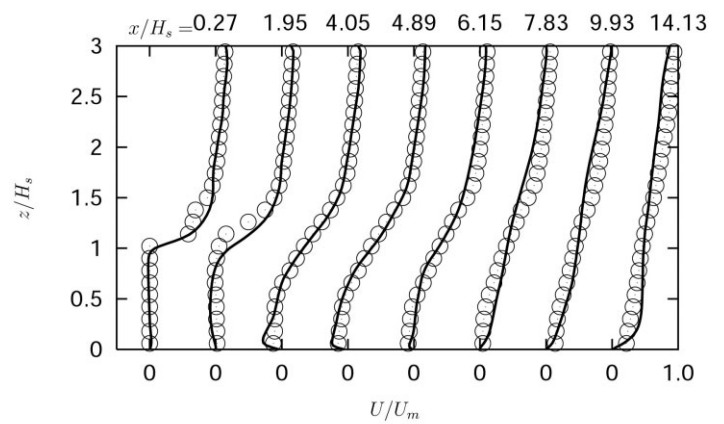


Figure 7 Mean velocity profile in flow past sudden drop in open channel, Case1. . present LES; . experiment by Maruyama(2002)

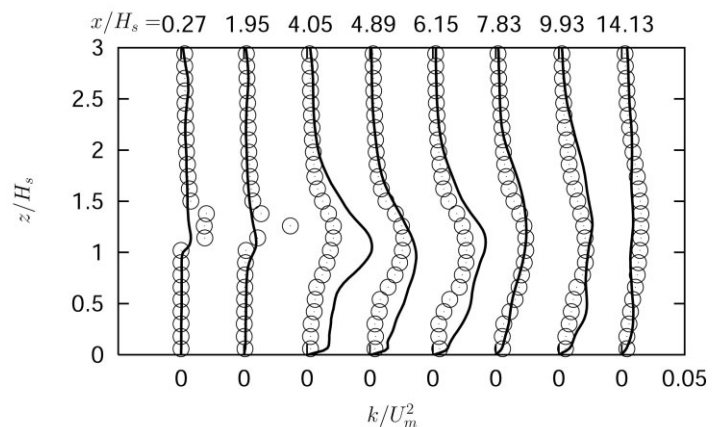


Figure 8 Turbulent kinetic energy in flow past sudden drop in open channel, Case1. . present LES; . experiment by Maruyama(2002)

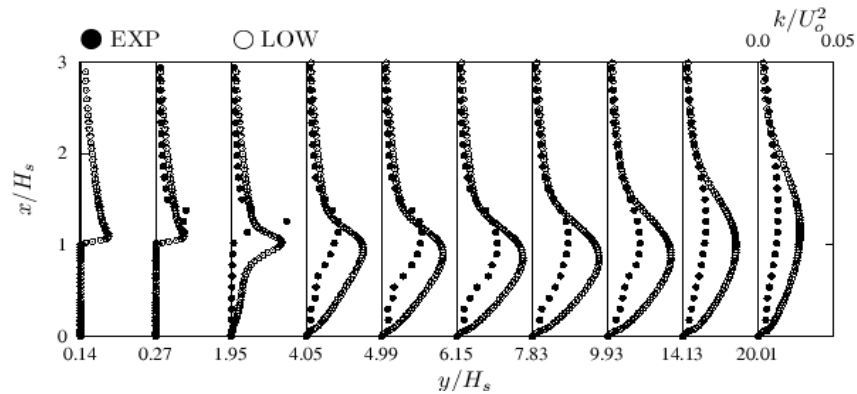


Figure 9 Turbulent kinetic energy in flow past sudden drop in open channel, Case1. k - ω method; \bullet , experiment by Maruyama(2002).

experimental data do not include the transverse fluctuations and should be somewhat smaller than the true kinetic energy but the plot indicates the LES is over-predicting k in most of the region. Since the experimental results also have some uncertainties, a conventional solution of the Reynolds-Averaged-Navier-Stokes (RANS) equations has also been conducted and is shown in Figure 9. It used the low Reynolds number k - ω turbulence model (Wilcox 1998). The present LES results and the RANS results are seen to agree very well except in the downstream recovery region.

Figure 10 shows the calculated average free-surface position for Case 1. It is plotted in terms of the deviation dH from the position right at the step. The plot is seen to be wiggly due to the fact that the free surface fluctuations are influenced by long-lasting waves that take a long time to converge. The magnitude of changes is too small to be seen in the mean-velocity plot of Figure 7. When the Froude number is low and the flow is subcritical, the free surface rises downstream of the step almost like the pressure in a closed channel. The amount of rise and the position where it takes the peak value are comparable to those reported by Nezu and Nakagawa (1993).

Figure 11 shows the distribution of the free-surface rms fluctuations. Again the results are wiggly indicating that it is even harder to obtain well-converged results. There is no data to verify these results but a little less than one percent of the step height, or about one third of the mean depth, is something that can be expected, say from a DNS

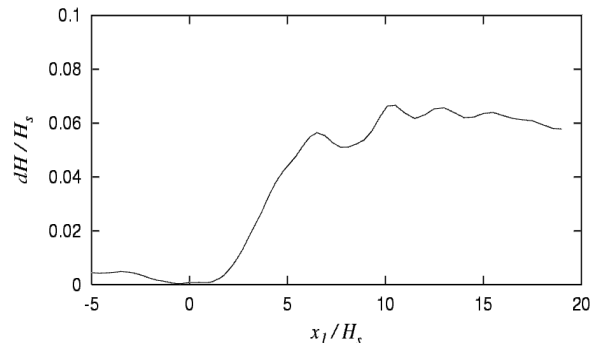


Figure 10 Calculated mean free-surface position.

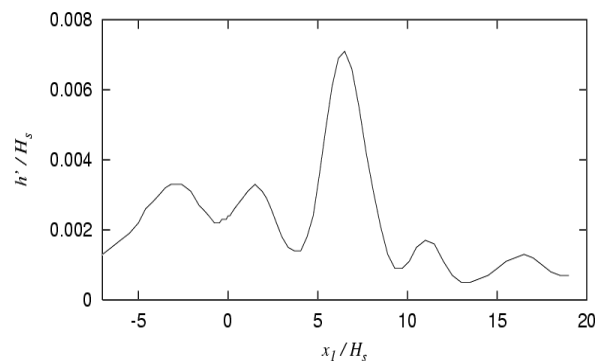


Figure 11 Calculated rms fluctuation level of the free surface.

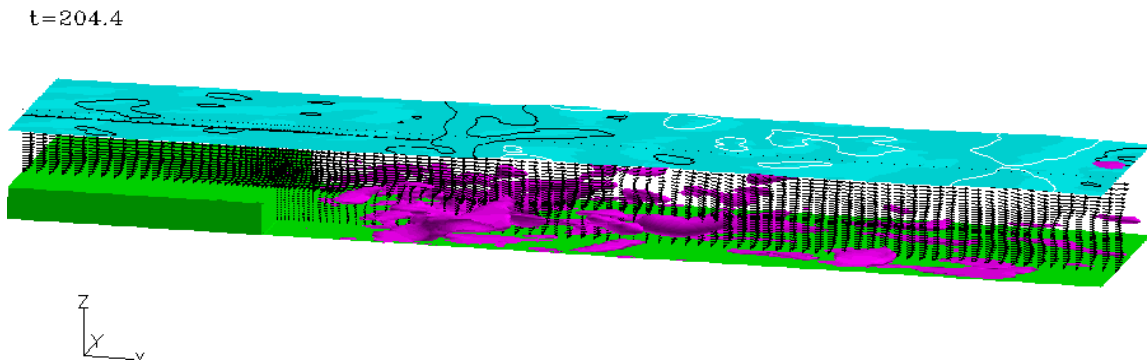


Figure 12 Instantaneous flow past sudden drop in open channel, Case1. arrows, velocity vectors in a vertical plane; lines on the free surface, free-surface elevation; pink surfaces, constant streamwise vorticity

calculation of Nakayama and Yokojima (2002). The peak fluctuation is seen at about seven step heights downstream of the step where the turbulent velocity fluctuations are the largest and this appears plausible.

The accuracy achieved by the current LES with marginal representation of the near-wall flow is not overwhelmingly better than those obtained with well-calibrated low-Reynolds number two-equation models. However, with the LES results, the instantaneous flow structures of large scale can be examined. Figure 12 shows an example of an instantaneous flow structure along with the velocity vectors in a vertical plane and the elevation of the free surface. The pink surfaces are the surfaces of constant streamwise component of the vorticity. The curves on the blue free surface indicate the elevation. The white curves show elevations higher than the mean and the black curves those lower than the mean. The figure indicates that, downstream of the step, there are some coherent vortex structures moving up towards the free surface where they interact with the swelling free surface. The scale of the free-surface undulations is seen to be about the same as those of these large vortex structures.

Figures 13 and 14 show calculation results of the mean velocity and turbulence kinetic energy for Case2, in which a weak hydraulic jump occurs and the free-surface rises by almost as much as the step height. Though there are no

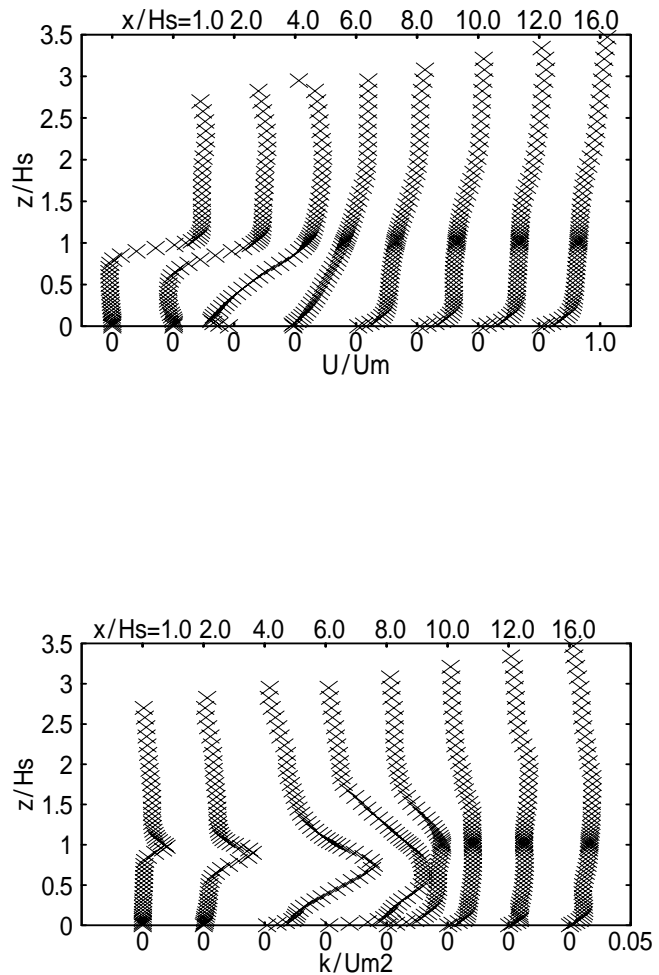


Figure 14 Turbulent kinetic energy in flow past sudden drop in open channel, Case2.

experimental data to compare and verify with this case, they show that the present calculation method can reproduce the large free-surface rise, the reduced separation length and large turbulence levels and indicate that the method can be applied to similar open-channel flows.

6. CONCLUSIONS

A large-eddy simulation method for open-channel flows with free-surface fluctuations has been developed and applied to several basic benchmark flows. Calculation of the free-surface motion is done by a modified HSMAC method and a standard Smagorinsky model for the sub-grid scale stress is used. The numerical grid must be fine enough so that there are a few points in the buffer layer where the sub-grid scale stress is damped. Those small-scale laboratory flume flows such as the fully developed open-channel flow or flow over a backward-facing step with mean depth of the order of a few centimeters can be adequately simulated with less than half a million grid points that can be handled by mid-grade personal computers. The mean-velocity results are accurately predicted. The prediction of the Reynolds stresses or the turbulent kinetic energy may not be overwhelmingly superior compared with a well calibrated RANS method, but the instantaneous large-scale turbulence structures are quite well reproduced, which can be useful in applications where sediment transport or scouring may become important.

REFERENCES

- Ferziger, J.H. and Peric, M.(1997). *Computational Methods for Fluid Dynamics*, Springer, Berlin.
- Hirt, C.W. and Cook, J.L.(1972). Calculating three-dimensional flow around structure and over rough terrain, *J. Comp. Phys.*, pp.324-340.
- Hirt, C.W. and Nichols, B.D.(1981). Volume of Fluid (VOF) method for the dynamics of free boundaries, *J. Comp. Phys.* Vol.39, pp.201-225.
- Hodges, B. R. and Street, R.L.(1999). On Simulation of Turbulent Nonlinear Free-Surface Flows, *J. Comp. Phys.*, Vol.151,
- Maruyama, T. (2002). Study of Open-channel Flow with Local Bed Variations, MS Thesis, Kobe University, Japan.
- Nakayama, T.(1997). Turbulent structures and characteristics of coherent vortices near the free-surface, MS thesis, Dept. Global Environment Engineering, Kyoto Univ., Japan.
- Nakayama, A. and Yokojima, S.(2001). Direct Numerical Simulation of the fully developed open-channel flow at subcritical Froude numbers, pp.569-576, DNS/LES progress and Challenges, Third AFOSR International Conference.
- Nakayama, A. and Vengadesan, S. N.(2002). On the influence of numerical schemes and subgrid-stress models on large-eddy simulation of turbulent flow past a square cylinder, *Int. J. Numerical Methods in Fluids*, Vol.38 No.3, pp.227-253.
- Nezu, I. and Nakagawa, (1993). *Turbulence in Open-Channel Flows*, A.A. Balkema, Rotterdam.
- Wilcox, D.C.(1998). *Turbulence Modeling for CFD*, DCW Industries, La Canada, California..
- Yabe, T. and Aoki, T.(1991). A universal solver for hyperbolic equations by cubic-polynomial interpolation I. One-dimensional solver, *Comput. Phys. Commun.*, Vol.66, pp.219-232.